Human Pathology (2019) **83**, 50–58

ELSEVIER

Human PATHOLOGY

www.elsevier.com/locate/humpath

Original contribution

Novel gene fusions in secretory carcinoma of the salivary glands: enlarging the *ETV6* family☆,☆☆,★,★★

Julie Guilmette MD, Dora Dias-Santagata PhD, Vânia Nosé MD, PhD, Jochen K. Lennerz MD, PhD, Peter M. Sadow MD, PhD*

Department of Pathology, Massachusetts General Hospital, Boston, MA 02114-2696, USA
Department of Pathology, Harvard Medical School, Boston, MA 02115, USA

Received 8 June 2018; revised 3 August 2018; accepted 9 August 2018

Keywords:
Secretory carcinoma;
Salivary gland tumor;
ETV6-NTRK3;
ETV6-RET;
MAML3

Summary Secretory carcinoma (SC) of the salivary gland is a low-grade malignancy associated with a well-defined clinical, histologic, immunohistochemical, and cytogenetic signature. Although the t(12;15) (p13; q25) translocation resulting in an *ETV6-NTRK3* gene fusion is well documented, advances in molecular profiling in salivary gland tumors have led to the discovery of *RET* as another *ETV6* gene fusion partner in SC. Here, we applied an RNA-based next-generation sequencing (NGS) approach for fusion detection on 14 presumed SC. The cases included 7 SC with classic *ETV6-NTRK3* gene fusion and 3 SC harboring *ETV6-RET* gene fusion. In addition, 2 cases revealed a *NCOA4-RET* gene fusion and were subsequently reclassified as intraductal carcinomas. One case with an unusual dual-pattern morphology revealed a novel translocation involving *ETV6*, *NTRK3*, and *MAML3* gene rearrangements. Interestingly, no *ETV6-NTRK3* or *ETV6-RET* SC was ever documented to have this unique dual-pattern morphology or harbor a *MAML3* mutation. The remaining case had no detected chromosomal abnormalities. Advances in molecular profiling of SC have led to the discovery of novel fusion partners such as *RET* and now *MAML3*. Further molecular characterization of salivary gland neoplasms is needed as these mutations may present alternative therapeutic targets in patients with these tumors.

1. Introduction

Since the initial description of secretory carcinoma (SC) of the salivary glands by Skálová et al [1], significant advances to characterize the immunophenotypic, cytogenetic, and ultrastructural profile of this entity have been performed [2-7]. A specific cytogenetic translocation t(12;15) (p13; q25) resulting in *ETV6-NTRK3* gene rearrangement was initially considered the distinct molecular signature of this tumor, although recent

☆ Competing interests: There are no conflicts of interest to report by any author.

☆☆ Funding/Support: This manuscript was funded by intradepartmental funding at Massachusetts General Hospital, including a Pathology Service Vickery Award to Drs Guilmette and Sadow.

★ Ethical Approval: This article does not contain any studies with human participants performed by the authors.

★★ Institutional Review Board Approval: This project was approved by the Massachusetts General Hospital Internal Review Board (P. M. Sadow, principal investigator; 2015P001749).

* Corresponding author at: Pathology Service, WRN219, Massachusetts General Hospital, 55 Fruit St, Boston, MA 02114-2696.
E-mail address: psadow@mgh.harvard.edu (P. M. Sadow).

https://doi.org/10.1016/j.humpath.2018.08.011
0046-8177/

studies have raised the possibility of alternative, unknown *ETV6* partners, *ETV6*-X [2,4]. In their study, Ito et al [4] have suggested a higher malignant potential among SC with unknown *ETV6* partners. Subsequently, one such alternative translocation resulting in an *ETV6-RET* gene rearrangement was documented in a subset of SC of the salivary glands [8]. The identification of this novel transcript promotes further molecular diversity in SC while opening the possibility of integrating targeted RET inhibitors as a potential therapeutic strategy [8].

After the identification of *ETV6-RET* gene rearrangements in 2 of our institutional cases of SC, an internal review was performed to further classify gene partners. In addition, patients' clinical profiles and progression were compared among different *ETV6* partners to stratify biological potential in SC with different *ETV6* partners.

2. Materials and methods

After approval from the institutional review board (2015P001749), 14 cases of SC of the salivary glands were retrieved from the pathology files of the Massachusetts General Hospital and Massachusetts Eye and Ear (Boston, MA) from 2003 to 2017. Consultation cases from referring institutions with no available slides were excluded. Hematoxylin and eosin (H&E)–stained slides along with ancillary studies and cytogenetic reports, in addition to patient medical records were reviewed.

2.1. Gene fusion analysis

Representative SC tumor foci were identified on H&E slides with corresponding areas selected from paraffin-embedded, formalin-fixed tissue blocks; nucleic acid was extracted and

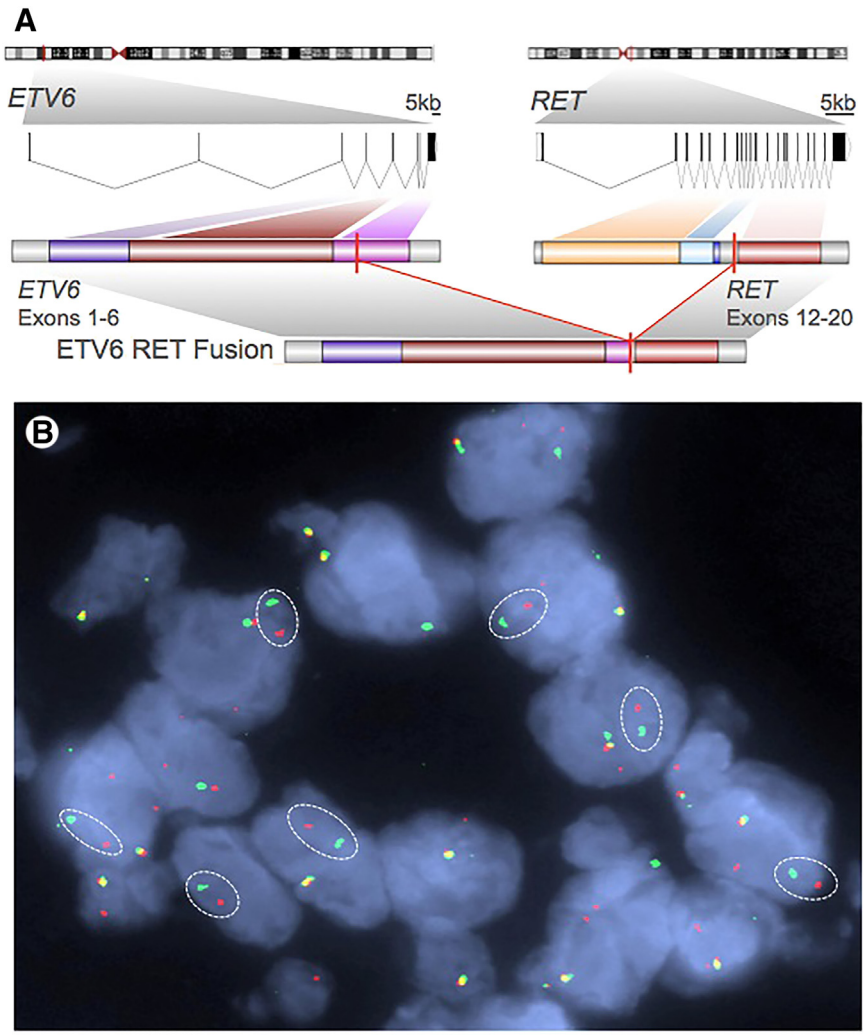

Fig. 1 *ETV6-RET* gene rearranged in SC of the salivary glands. A, Genomic exon structure of the fusion and predicted *ETV6-RET* fusion protein. Domains indicated by colors: *ETV6*: purple, helix-loop-helix domain; red, internal domain; pink, *ETS* domain; *RET*: yellow, cadherin domains; blue, cysteine-rich domain; purple, transmembrane domain; red, kinase domains 1 + 2. B, FISH of interphase nuclei showing isolated 3′ (red)-probe and 5′ (green)-probe signals in the tumor cells (ovals).

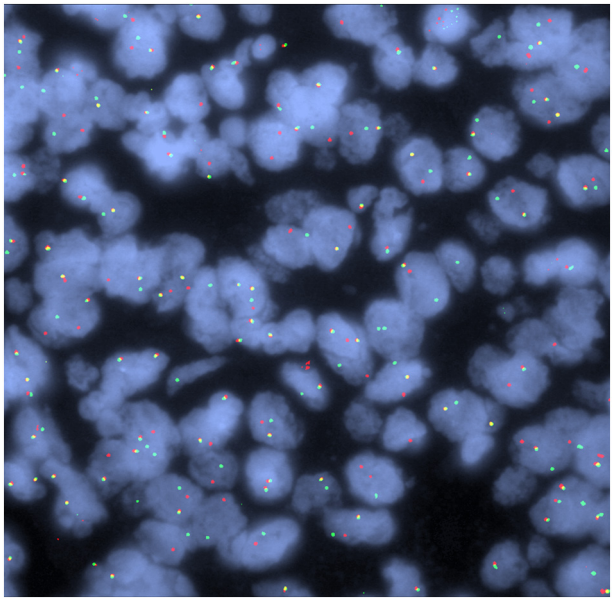

Fig. 2 Interphase FISH analysis using dual-color break-apart probe for *NTRK3* (15q25) gene reveals 1 non-rearranged orange/green fusion signal, 1 orange signal, and 1 separate green signal indicating the translocation of *NTRK3* in all tumor cells.

analyzed for rearrangements using a targeted next-generation sequencing (NGS) assay based on anchored multiplex polymerase chain reaction, as previously described [9]. The fusion assay (FusionPlex Solid Tumor Kit; ArcherDX Inc, Boulder, CO) was designed to detect fusion transcripts in reverse-transcribed double-stranded complementary DNA (cDNA) and to target 53 cancer genes. Total nucleic acid was isolated from formalin-fixed, paraffin-embedded tumor specimens and reverse transcribed with random hexamers, followed by second-strand synthesis to create double-stranded cDNA. The double-stranded cDNA was end-repaired, adenylated, and ligated with a half-functional adapter. Two hemi-nested polymerase chain reactions were applied to create a fully functional sequencing library. Illumina MiSeq 2 (Illumina Incorporated, San Diego, CA) paired-end sequencing results were aligned to the hg19 reference genome [9,10]. A laboratory-developed algorithm was used for fusion transcript detection and annotation. The integrity of the input nucleic acid and the technical performance of the assay were evaluated with control sequences from the *B2M*, *CTBP1*, and *GAPDH* targets. The assay is validated for samples with 5% or higher tumor cellularity. This analysis was successfully performed on all 14 specimens.

2.2. Detection of alteration of *NTRK3* by fluorescence in situ hybridization

For one case (case 11), fluorescence in situ hybridization (FISH) using a dual-color break-apart probe for *NTRK3* (15q25) gene was performed on 5-µm unstained sections prepared from the archival tissue block used for both NGS analysis and immunohistochemistry. The LSI *NTRK3* (15q25) Dual-Color Break-Apart Rearrangement Probe (Abbott Molecular, Des Plaines, IL) was used to confirm the loci of interest. Slides were pretreated using an automated VP 2000 processor (Abbott Molecular) following the manufacturer's protocols. Cellular DNA and probes were codenatured at 76°C for 10 minutes using the ThermoBrite system (Abbott Molecular) and incubated overnight at 37 °C in a humidified chamber. Nuclei were stained with 4,6-diamidino-2-phenylindole in Antifade solution (Abbott Molecular), and slides were analyzed using a Leica DM6000B fluorescence microscope (Leica Microsystems, Buffalo Grove, IL). Hybridization signals were examined in 50 to 100 interphase tumor nuclei per specimen. Images were taken and stored using the CytoVision Image Analysis System (Genetix, San Jose, CA).

2.3. Immunohistochemistry

Immunohistochemical studies were performed on 5-µm-thick sections of formalin-fixed, paraffin-embedded tissue in a Bond 3 automated immunostainer (Leica Microsystems, Bannockburn, IL) and primary antibodies against S100 protein (Ventana, Oro Valley, AZ; prediluted), mammaglobin (Dako; 1:250), and DOG1 (Dako, Santa Clara, CA; prediluted). Appropriate positive and negative controls were included. No significant background staining was seen in the negative cases.

3. Results

3.1. Molecular profile

Fourteen cases of SC of the salivary glands were analyzed by NGS fusion assay using the SNaPshot multiplexed targeted platform. Among these cases, 7 tumors showed fusion transcripts involving *ETV6* exon 5 (ENST00000396373) and *NTRK3* exon 15 (ENST00000360948). Three cases demonstrated fusion transcripts involving *ETV6* exon 6 (ENST00000396373) and *RET* exon 12 (ENST00000355710) (Fig. 1A and B). One case revealed fusion transcripts involving *ETV6* exon 5 (ENST00000396373) and *NTRK3* exon 15 (ENST00000360948) and a separate fusion between *ETV6* exon2 (ENST00000396373) and *MAML3* exon 2 (ENST00000509479). The H&E slides for this case were reassessed. Two morphologically distinct architectural patterns were intermixed within the same tumor. Both areas were labeled and resubmitted separately for NGS analysis. The data obtained from the second sequencing revealed that both areas are molecularly identical and harbored the same 2 previously mentioned fusion transcripts. FISH using a dual-color break-apart probe for *NTRK3* (15q25) gene confirmed the presence of *NTRK3* rearrangement in both areas, suggesting a biphasic or dual-patterned tumor (Fig. 2). Two other tumors showed fusion transcripts for *RET* exon 12 (ENST00000355710) and *NCOA4* exon 6 (ENST00000452682). A final case revealed no translocation on our molecular fusion assay (Table).

Table Clinical information on patients with secretory carcinoma and intraductal carcinom of the salivary glands

Patients	Age (y)	Sex	Tumor location	Tumor size (cm)	Tumor extension	IHC	Follow-up
t(12;15), *ETV6-NTRK3* (SC)							
1	55	M	Parotid	3.5	No LVI No PNI 0/1	S100+ Mam+ DOG1−	No recurrence (6 y)
2	33	F	Parotid	2.4	No LVI No PNI 0/5	S100+ Mam+ DOG1−	No recurrence (4 y)
3	64	F	Buccal mucosa	0.6	LVI+ No PNI	S100+ Mam+ DOG1−	No recurrence (3 y)
4	45	F	Parotid	1.8	No LVI No PNI	S100+ Mam+ DOG1−	No recurrence (15 y)
5	34	F	Parotid	4.0	No LVI No PNI	S100+ Mam+ DOG1−	No recurrence (3 y)
6	21	M	Palate	0.8	No LVI No PNI	S100+ Mam+ DOG1−	No recurrence (2 y)
7	55	M	Buccal mucosa	0.5	No LVI No PNI	S100+ Mam+ DOG1−	No recurrence (1 y)
t(10;12), *ETV6-RET* (SC)							
8	42	M	Parotid	2.9	LVI+ Infiltrates skeletal muscle No PNI 0/11	S100+ Mam+ DOG1−	No recurrence (4 y)
9	68	M	Submandibular gland	1.5	No LVI No PNI	S100+ Mam+ focal DOG1−	Prior submandibular tumor, 1996 (1 y)
10	54	F	Parotid	3.0	LVI+ Metastases: lungs, bones, pleural/pericardial effusion	S100+ Mam+ DOG1−	Deceased
ETV6, *NTRK3*, and *MAML3* gene rearrangements (SC)							
11	40	M	Parotid	0.8	LVI+ No PNI 6/33	S100+ Mam+ Focal DOG1−	No recurrence (1 y)
No translocation detected (SC)							
12	76	F	Parotid	2.3	No LVI No PNI 0/11	S100+ Mam+ DOG1−	No recurrence (1 y)
t(10;12), *NCOA4-RET* (IC)							
13	44	F	Parotid	1.1	No LVI No PNI	S100+ Mam+ DOG1−	No recurrence (3 y)
14	88	F	Parotid	2.2	No LVI No PNI	S100+ Mam+ DOG1−	No recurrence (1 y)

Abbreviations: M, male; F, female; LVI, lymphovascular invasion; PNI, perineural invasion; IHC, immunohistochemistry; Mam, mammaglobin.

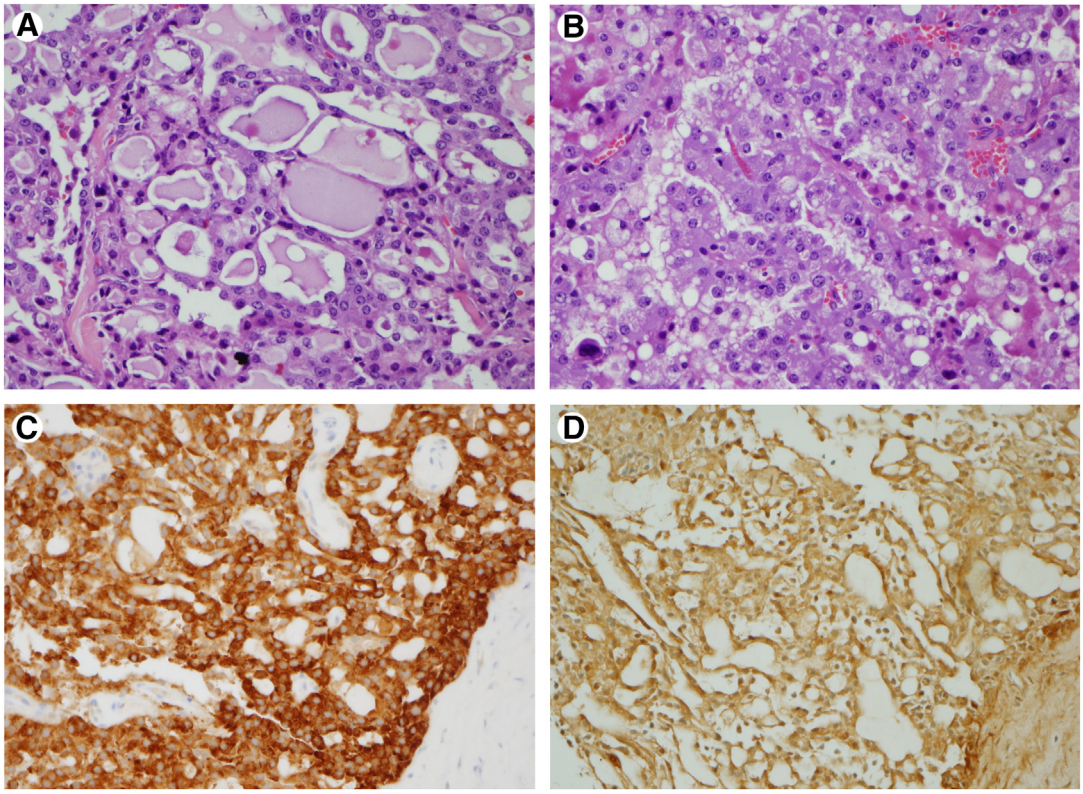

Fig. 3 A, Histology of SC with classic *ETV6-NTRK3* gene fusion demonstrates a microcystic/cribriform growth pattern with occasional papillary architecture (B) with "bubbly" eosinophilic secretory material (H&E stain, original magnification ×400). The tumors cells show strong, diffuse staining for both mammaglobin (C) and S100 proteins (D; ×200).

3.2. Clinical and histologic characteristics of *ETV6-NTRK3* SC

The clinical and follow-up data of the 7 patients with *ETV6-NTRK3* SC are summarized in Table, which includes 3 men and 4 women with a mean age of 44 years, ranging from 21 to 64 years. Four of the tumors are in parotid glands and the remainder in minor salivary glands. Recorded tumor size is variable and ranges from 0.6 to 4.0 cm in largest diameter (mean of 1.9 cm). The tumors are either encapsulated or well-circumscribed within the salivary gland with occasional limited/focal extension into the perisalivary soft tissue. The tumors have an invasive lobulated growth pattern separated by thin fibrous septa. Histologically, all tumors show typical SC features with one or more of microcystic, tubular, follicular, solid, and papillary-cystic architectural patterns and characteristic secretory eosinophilic material (Fig. 3A and B). The neoplastic cells contain eosinophilic finely granulated or vacuolated cytoplasm with a round-to-ovoid nuclei. Except for one tumor, which shows lymphovascular invasion (case 3), all other tumors have no lymphovascular or perineural invasion. There are no features suggestive of high-grade transformation. Although no cervical lymph node dissections were performed in any of the 7 cases, lymph nodes identified within the main specimens showed no evidence of metastatic disease (cases 1 and 2). In all cases, tumor cells displayed strong, diffuse staining for both mammaglobin (Fig. 3C) and S100 proteins (Fig. 3D) along with negative DOG1 staining. Clinical follow-up ranged from 1 to 15 years with no local recurrence, lymph node, or distant metastasis reported in any of these patients.

3.3. Clinical and histologic characteristics of *ETV6-RET* SC

Among the 3 cases of SC with *ETV6-RET* translocation, 2 men and 1 woman were identified ranging from 42 to 68 years old (Table). Two tumors arose in the parotid and 1 in the submandibular gland. The recorded tumor size varied from 1.5 to 3.0 cm. Histologic features were almost identical to those previously described above in *ETV6-NTRK3* SC (Fig. 4). Two cases (cases 8 and 10) showed lymphovascular invasion but no perineural invasion. In 1 patient (case 8), SC infiltrated into adjacent skeletal muscle. Ipsilateral neck dissection did not reveal any metastatic disease. Another patient (case 9) presented with an unusual medical history. This patient presented with a slowly progressive left submandibular neck mass in 1996 in Vietnam. A submandibular gland excision was performed, and the patient was treated with radiotherapy. Twenty-one years later, the patient re-presented for a similar left submandibular mass. Surgical resection revealed SC surrounded by scar tissue consistent with prior surgery. Tumor cells showed strong, diffuse positivity for S100 protein but only focal

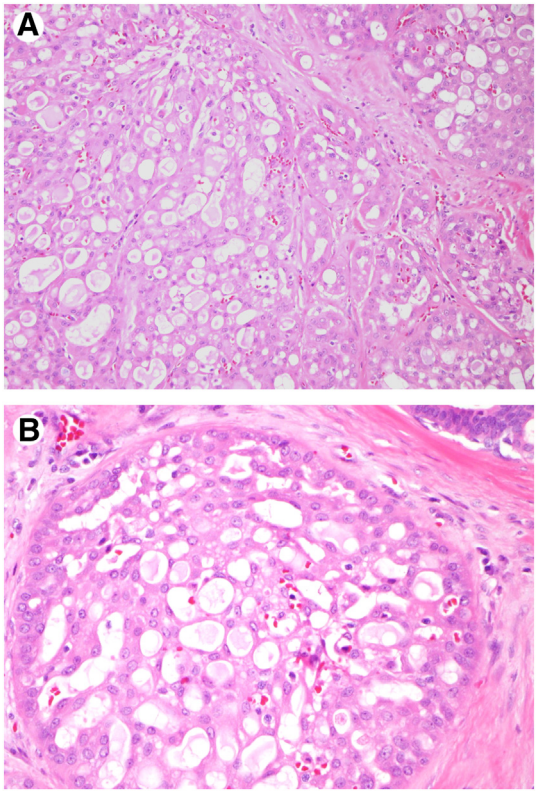

Fig. 4 Histology of SC with *ETV6-RET* translocation showing the typical cribriform architecture with low-grade nuclear atypia and intraluminal eosinophilic secretory material (H&E stain, original magnification ×200).

mammaglobin expression. The patient did not recall the initial tumor diagnosis, and medical reports from the outside institution were not available. In case 10, the patient presented at an advanced stage with distant metastases to the lungs and bones, in addition to pleural and pericardial carcinomatous effusion, confirmed by fine needle aspiration. NGS fusion assay was requested on the initial tumor at the time of diagnosis, and *ETV6-RET* translocation was identified. This patient's treatment strategy included kinase inhibitors targeting *RET* mutation. Because of the advanced disease, the patient died within a year of diagnosis and tumor response to treatment was not documented.

3.4. Clinical and histologic characteristics of the dual-fusion *ETV6-NTRK3* and *ETV6-MAML3* SC

Case 11 represents a 40-year-old man with a 0.8-cm parotid mass associated with ipsilateral adenopathy. Histologically, the tumor revealed dichotomous growth patterns. One area of the tumor had tubular and solid architecture with neoplastic cells containing finely granulated eosinophilic cytoplasm and round-to-ovoid nuclei (Fig. 5A-C). Here, the tumor was diffusely positivity for S100 protein with only focal mammaglobin expression (Fig. 5D and E). DOG1 immunostain was negative. The second component of the tumor had cribriform and papillary architecture with pseudostratified cuboidal-to-columnar cells. This distinct tumor component had clear-to-amphophilic cytoplasm with basally oriented nuclei. The nuclei had irregular nuclear contours with chromatin clearing and small nucleoli. Dense eosinophilic secretory material was frequently observed. Mitotic activity was quite low with very focal necrosis. In addition to S100 protein, mammaglobin, and DOG1, initial immunohistochemical studies included p63, TTF1, thyroglobulin, CD117, MYB, and androgen receptor, which were all negative. Only immunostains for pankeratins, including AE1/AE3 and CAM5.2, were observed in both distinct morphologic areas with variable intensity (Fig. 5F). Taken together, the morphologic, immunohistochemical, and molecular phenotype of this tumor was consistent with a dual-patterned SC.

3.5. Clinical and histologic characteristics of *NCOA4-RET* carcinoma

Two patients aged 44 and 88 years had *NCOA4-RET* gene fusions in carcinomas arising in the parotid gland. Both cases were reassessed and revealed similar histologic features to SC including microcystic, cribriform, and papillary architecture with eosinophilic secretory material and low-grade nuclear features. Rather than forming mass-like lesions, tumor nests appeared more dispersed and centered on salivary ducts (Fig. 6A). A prominent lymphoplasmacytic inflammatory infiltrate and fibrosis surrounded tumor islands. Immunohistochemistry revealed tumor cells to be positive for S100 and mammaglobin but negative for DOG1. Additional studies performed showed that tumor nests were surrounded by a rim of p63-positive myoepithelial cells (Fig. 6B) corresponding to the salivary duct lining. No invasive component was identified. Immunostain for androgen receptor was negative in both cases. Based on both histology and immunohistochemistry, these 2 tumors were reclassified as intraductal carcinoma (IC), low-grade.

3.6. Clinical and histologic characteristics of carcinoma with no identified translocation

One case (case 12) features a 76-year-old woman with a 2.3-cm parotid mass. The tumor morphology had characteristic microcystic and papillary-cystic architecture associated with secretory eosinophilic intraluminal material, as previously described in SC. Neoplastic cells contained finely granulated eosinophilic cytoplasm with low-grade nuclei. There was no evidence of lymphovascular invasion, perineural invasion, or cervical lymph node metastases. The tumor cells were diffusely positive for mammaglobin and S100 expression but negative for DOG1 and p63.

4. Discussion

Although *ETV6-NTRK3* gene fusion is canonical for SC, advances in molecular profiling of this tumor have led to the

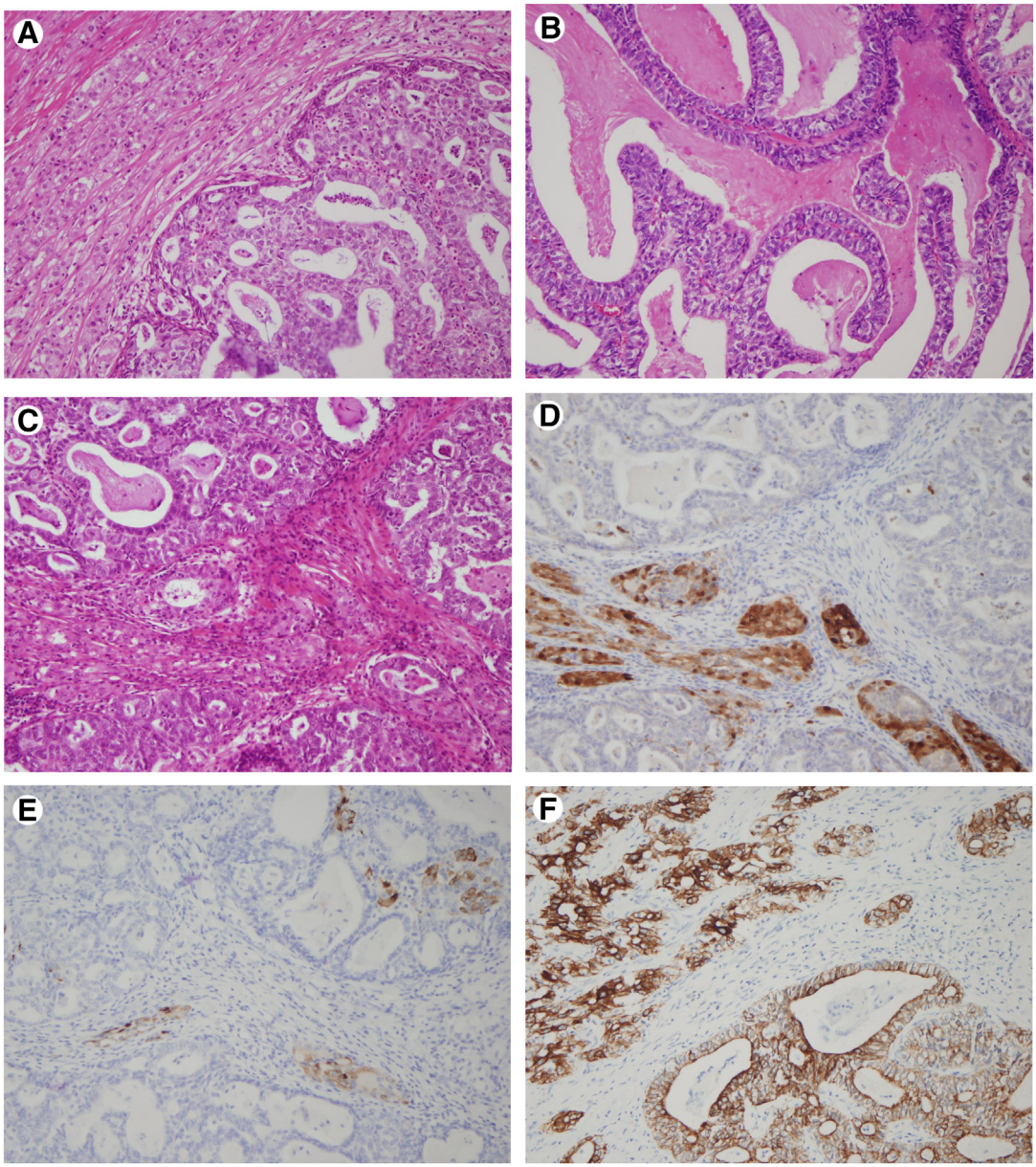

Fig. 5 Dual-patterned SC with *ETV6*, *NTRK3*, and *MAML3*. A, Tumor with 2 distinct growth patterns; one area showing "typical SC" tubular and solid architecture with low-grade morphology (upper left), and the other comprises cribriform and papillary patterns. B, In the second area, the tumor cells are pseudostratified with cuboidal-to-columnar cells containing clear-to-amphophilic cytoplasm and atypical nuclei. Dense eosinophilic secretory material is observed. C, Frequently, both morphologies are admixed (A-C, H&E stain, original magnification ×200). The typical SC stains for S100 protein (D) but only focally for mammaglobin (E), whereas the other area is completely negative for both stains. F, Only immunostain for CKAE1/AE3/CAM5.2 was observed in both areas with variable intensity, stronger intensity in the "typical SC" and moderate intensity in the cribriform area (D-F, ×200).

discovery of novel *ETV6* fusion partners, such as *RET* and now *MAML3*. The *ETV6-RET* translocation was just recently described by Skálová et al [8] in 2018. In their analysis of 10 cases, the morphologic and immunohistochemical findings in both tumor groups, *ETV6-NTRK3* SC and *ETV6-RET* SC, were practically identical [8]. Our results support a similar conclusion. Although our analysis is mitigated by our small sample size and lacks statistical significance, the *ETV6-RET* SC group seemed to exhibit more aggressive biological features. Two of the 3 cases had lymphovascular invasion, whereas 1 case showed infiltration into the adjacent skeletal muscle and another presented with multisystemic metastatic disease. Our results corroborate the previous study by Ito et al [4], suggesting that SC with alternate *ETV6* partners may be more biologically aggressive. The identification of *ETV6* partners may contribute to therapeutic management of patients with advanced disease. Patients with SC featuring *ETV6-NTRK3* gene rearrangement can benefit from NTRK3-

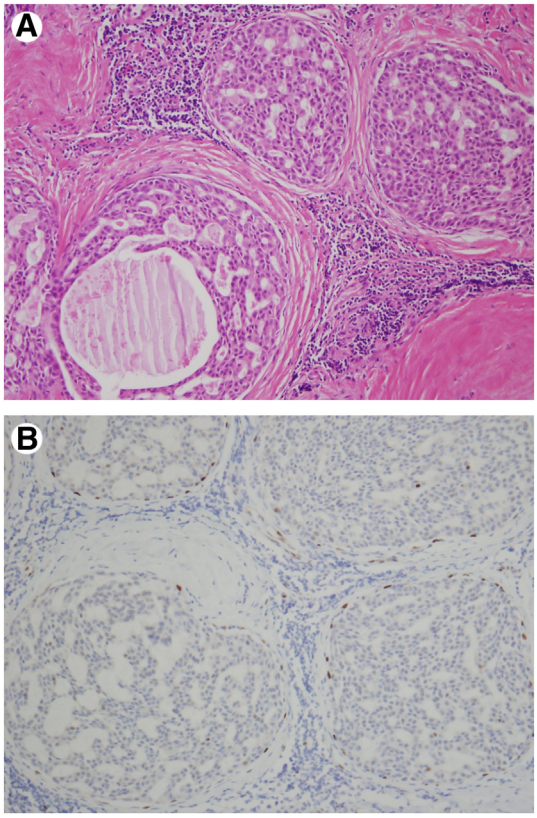

Fig. 6 IC with *NCOA-RET* translocation has microcystic and cribriform architecture (A) with low-grade nuclear features. Tumor nests are associated with a lymphoplasmacytic infiltrate and fibrosis (H&E stain, original magnification ×200). Immunohistochemistry demonstrates a rim of p63-positive myoepithelial cells (B) surrounding each tumor nest (×200).

targeted therapy, whereas those with SC *ETV6-RET* gene rearrangement can be considered for potential *RET* inhibitors [8,11,12].

To our knowledge, dual-patterned SC harboring dual *ETV6-NTRK3* and *ETV6-MAML3* gene fusions has not been reported in the salivary glands until now. Thorough molecular analysis using a targeted NGS-based fusion assay in combination with FISH dual-color break-apart probes for *NTRK3* gene confirmed the presence of both fusion transcripts in all tumor cells, regardless of the 2 distinct architectural patterns and morphologies. The actual nature of the translocations remains unclear but most likely involves 2 chromosomal rearrangements leading to the production of 2 different fusion proteins, *ETV6-NTRK3* and *ETV6-MAML3*. Protein expression from the unusual combination of these fusion transcripts certainly would affect even the standard aberrant cell programming seen in SC [13-15]. As a result, distinct architectural, histologic, and immunohistochemical phenotypic expression might expectedly emerge within the same tumor. Although unusual, it has been documented in few head and neck malignancies, such as biphenotypic sinonasal sarcoma (BSNS) [16-19]. In BSNS, the term "biphenotypic" refers to the dual immunohistochemical expression of neural and smooth muscle markers with a uniform population of spindled cells, whereas in our case, we use "dual-patterned" to imply distinct morphologic and immunohistochemical expression found within 2 distinct epithelial components of the tumor. BSNS is a low-grade sarcoma that exhibits both neural and myogenic differentiation resulting from recurrent rearrangements in *PAX3* gene, a transcription factor that promotes interactions in cell differentiation of both lineages [16,20]. Among the documented genes partnered with *PAX3* in BSNS, *PAX3-MAML3* gene fusion has been identified as a recurrent translocation partner [21]. *MAML3* is a member of the mastermind-like (MAML) family of transcriptional co-activators for the Notch signaling pathway, which takes part in a variety of cellular interactions, including cell differentiation, proliferation, and death [22,23]. Although it remains unclear how *MAML3* modulates the oncogenic function of *PAX3*, it has been hypothesized that *MAML3* could function as a potent transcriptional activator of *PAX3* response elements [21]. Unlike BSNS, only the epithelial cell lineage has been identified in our case. The mechanistic role of the 2 transcripts, *ETV6-NTRK3* and *ETV6-MAML3*, still needs to be elucidated. Of note, no *ETV6-NTRK3* or *ETV6-RET* SC was ever documented to have a dual-patterned morphology.

Interestingly, 2 cases of IC (cases 13 and 14) were initially classified as SC in our sample group. Although these 2 cases might have been eliminated from our study retrospectively, from a clinical, morphologic, and immunohistochemical standpoint, IC is a potent mimicker of SC often requiring a thorough workup to reach the appropriate diagnosis. In our 2 cases, the identification of *NCOA4-RET* gene rearrangement was the key feature that led to the diagnosis of IC, and for this reason, these cases remained included in our study. IC is a rare salivary gland tumor characterized mainly by intraductal epithelial proliferation with low-, intermediate-, or high-grade nuclear atypia and may occasionally show microinvasion into the surrounding tissue [24-27]. Rare cases with widespread invasion have been documented, which has led to question a potential relationship between IC and salivary duct carcinoma [28,29]. Recently, a novel *NCOA4-RET* fusion was identified in a subset of IC with intercalated duct morphology [30], which also corroborates with our findings. IC is an undeniable mimicker of SC, as both share a similar morphology and expression of both S100 and mammaglobin immunostains [31]. Distinction of these 2 malignancies can made histologically by the identification of a nonneoplastic myoepithelial layer surrounding the tumor nests exposing the in situ component in IC [29]. Advances in molecular characterization of salivary gland tumors have allowed to further stratify these neoplasms by their molecular signature such as *ETV6* gene rearrangements for SC and recurrent *RET* rearrangements in the case of IC [29,32,33].

One case (case 12) in our cohort did not reveal any translocations targeted by our assay. This case was reviewed by 2 senior head and neck pathologists (P. S. and V. N.). The combination of histology, immunohistochemistry, and molecular findings were compatible with a low-grade

adenocarcinoma of the salivary glands. The diagnosis of SC in the absence of an *ETV6* translocation may be perceived as highly controversial, although rare cases have been previously described [34,35].

In addition to *NTRK3*, the recent discovery of variable fusion partners in SC such as *RET* and now *MAML3* might present alternative molecular pathways to consider for opportune therapeutic targets in patients with advanced or recurrent disease. These findings provide novel insight into the oncogenesis, histopathology, and molecular diagnosis of this newly recognized carcinoma, putative family of carcinomas, of the salivary glands.

References

[1] Skálová A, Vanecek T, Sima R, et al. Mammary analogue secretory carcinoma of salivary glands, containing the etv6-ntrk3 fusion gene: a hitherto undescribed salivary gland tumor entity. Am J Surg Pathol 2010;34:599-608.

[2] Skálová A, Vanecek T, Simpson RHW, et al. Mammary analogue secretory carcinoma of salivary glands: molecular analysis of 25 ETV6 gene rearranged tumors with lack of detection of classical ETV6-NTRK3 fusion transcript by standard RT-PCR. Am J Surg Pathol 2016;40:3-13.

[3] Bishop JA. Unmasking MASC: bringing to light the unique morphologic, immunohistochemical and genetic features of the newly recognized mammary analogue secretory carcinoma of salivary glands. Head Neck Pathol 2013;7:35-9.

[4] Ito Y, Ishibashi K, Masaki A, et al. Mammary analogue secretory carcinoma of salivary glands: a clinicopathologic and molecular study including 2 cases harboring ETV6-X fusion. Am J Surg Pathol 2015;39:602-10.

[5] Guilmette J, Nielsen GP, Faquin WC, et al. Ultrastructural characterization of mammary analogue secretory carcinoma of the salivary glands: a distinct entity from acinic cell carcinoma? Head Neck Pathol 2017;11:419-26.

[6] Skalova A. Mammary analogue secretory carcinoma of salivary gland origin: an update and expanded morphologic and immunohistochemical spectrum of recently described entity. Head Neck Pathol 2013;7:30-6.

[7] Patel KR, Solomon IH, El-Mofty SK, Lewis JS, Chernock RD. Mammaglobin and S-100 immunoreactivity in salivary gland carcinomas other than mammary analogue secretory carcinoma. Hum Pathol 2013;44:2501-8.

[8] Skalova A, Vanecek T, Martinek P, et al. Molecular profiling of mammary analog secretory carcinoma revealed a subset of tumors harboring a novel ETV6-RET translocation: report of 10 cases. Am J Surg Pathol 2018;42:234-46.

[9] Kent WJ. BLAT—the BLAST-like alignment tool. Genome Res 2002;12:656-64.

[10] Li H, Durbin R. Fast and accurate short read alignment with Burrows-Wheeler transform. Bioinformatics 2009;25:1754-60.

[11] Chi HT, Ly BTK, Kano Y, Tojo A, Watanabe T, Sato Y. ETV6-NTRK3 as a therapeutic target of small molecule inhibitor PKC412. Biochem Biophys Res Commun 2012;429:87-92.

[12] Wang K, Russell JS, McDermott JD, et al. Profiling of 149 salivary duct carcinomas, carcinoma ex pleomorphic adenomas, and adenocarcinomas, not otherwise specified reveals actionable genomic alterations. Clin Cancer Res 2016;22:6061-8.

[13] Bene MC. Biphenotypic, bilineal, ambiguous or mixed lineage: strange leukemias. Haematologica 2009;94:891-3.

[14] Steensma DP. Oddballs: acute leukemias of mixed phenotype and ambiguous origin. Hematol Oncol Clin North Am 2011;25:1235-53.

[15] Weinberg OK, Arber DA. Mixed-phenotype acute leukemia: historical overview and a new definition. Leukemia 2010;24:1844-51.

[16] Rooper LM, Huang SC, Antonescu CR, Westra WH, Bishop JA. Biphenotypic sinonasal sarcoma: an expanded immunoprofile including consistent nuclear β-catenin positivity and absence of SOX10 expression. Hum Pathol 2016;55:44-50.

[17] Zhao M, LaoI QY, Zhao DH, et al. Clinicopathologic and molecular genetic characterizations of biphenotypic sinonasal sarcoma. Chin J Pathol 2017;46:841-6.

[18] Kakkar A, Rajeshwari M, Sakthivel P, Sharma MC, Sharma SC. Biphenotypic sinonasal sarcoma: a series of six cases with evaluation of role of β-catenin immunohistochemistry in differential diagnosis. Ann Diagn Pathol 2018;33:6-10.

[19] Bishop JA. Recently described neoplasms of the sinonasal tract. Semin Diagn Pathol 2016;33:62-70.

[20] Wang Q, Fang WH, Krupinski J, Kumar S, Slevin M, Kumar P. Pax genes in embryogenesis and oncogenesis. J Cell Mol Med 2008;12:2281-94.

[21] Wang X, Bledsoe KL, Graham RP, et al. Recurrent PAX3-MAML3 fusion in biphenotypic sinonasal sarcoma. Nat Genet 2014;46:666-8.

[22] Lin SE, Oyama T, Nagase T, Harigaya K, Kitagawa M. Identification of new human mastermind proteins defines a family that consists of positive regulators for notch signaling. J Biol Chem 2002;277:50612-20.

[23] McElhinny AS, Li JL, Wu L. Mastermind-like transcriptional coactivators: emerging roles in regulating cross talk among multiple signaling pathways. Oncogene 2008;27:5138-47.

[24] Chen K. Intraductal carcinoma of the minor salivary gland. J Laryngol Otol 1983;97:189-91.

[25] Delgado R, Klimstra D, Albores-Saavedra J. Low grade salivary duct carcinoma: a distinctive variant with a low grade histology and a predominant intraductal growth pattern. Cancer 1996;78:958-67.

[26] Brandwein-Gensler M, Hille J, Wang BY, et al. Low-grade salivary duct carcinoma: description of 16 cases. Am J Surg Pathol 2004;28:1040-4.

[27] Cheuk W, Chan JKC. Advances in salivary gland pathology. Histopathology 2007;51:1-20.

[28] Weinreb I, Tabanda-Lichauco R, Van Der Kwast T, Perez-Ordoñez B. Low-grade intraductal carcinoma of salivary gland: report of 3 cases with marked apocrine differentiation. Am J Surg Pathol 2006;30:1014-21.

[29] Weinreb I. Intraductal carcinoma of salivary gland (so-called low-grade cribriform cystadenocarcinoma) arising in an intraparotid lymph node. Head Neck Pathol 2011;5:321-5.

[30] Weinreb I, Bishop JA, Chiosea S, et al. Recurrent RET gene rearrangements in intraductal carcinomas of salivary gland. Am J Surg Pathol 2018;42:442-52.

[31] Stevens TM, Kovalovsky AO, Velosa C, et al. Mammary analog secretory carcinoma, low-grade salivary duct carcinoma, and mimickers: a comparative study. Mod Pathol 2015;28:1084-100.

[32] Fonseca FP, Sena Filho M, Altemani A, Speight PM, Vargas PA. Molecular signature of salivary gland tumors: potential use as diagnostic and prognostic marker. J Oral Pathol Med 2016;45:101-10.

[33] Chiosea SI, Griffith C, Assaad A, Seethala RR. Clinicopathological characterization of mammary analogue secretory carcinoma of salivary glands. Histopathology 2012;61:387-94.

[34] Shah AA, Wenig BM, LeGallo RD, Mills SE, Stelow EB. Morphology in conjunction with immunohistochemistry is sufficient for the diagnosis of mammary analogue secretory carcinoma. Head Neck Pathol 2015;9:85-95.

[35] Dogan S, Arcila M, Berger D, Katabi N. Carcinoma of salivary glands reveals novel *NCOA4-RET* fusion in mammary analog secretory carcinoma. Abstract 1298. Mod Pathol 2017;30(Suppl):323A.